ADVANCES IN ATMOSPHERIC SCIENCES, VOL. 39, MARCH 2022, 403–414

• **Original Paper** •

A New Index Developed for Fast Diagnosis of Meteorological Roles in Ground-Level Ozone Variations

Weihua CHEN[1], Weiwen WANG[1], Shiguo JIA[2], Jingying MAO[1], Fenghua YAN[1], Lianming ZHENG[1], Yongkang WU[1], Xingteng ZHANG[1], Yutong DONG[1], Lingbin KONG[1], Buqing ZHONG[3], Ming CHANG[1], Min SHAO[1], and Xuemei WANG[*1]

[1]*Guangdong-Hongkong-Macau Joint Laboratory of Collaborative Innovation for Environmental Quality, Institute for Environmental and Climate Research, Jinan University, Guangzhou* 510632, *China*

[2]*School of Atmospheric Sciences, Guangdong Province Key Laboratory for Climate Change and Natural Disaster Studies, Sun Yat-sen University, Guangzhou* 510275, *China*

[3]*Key Laboratory of Vegetation Restoration and Management of Degraded Ecosystems, South China Botanical Garden, Chinese Academy of Sciences, Guangzhou* 510650, *China*

(Received 6 July 2021; revised 8 September 2021; accepted 8 October 2021)

ABSTRACT

China experienced worsening ground-level ozone (O_3) pollution from 2013 to 2019. In this study, meteorological parameters, including surface temperature (T_2), solar radiation (SW), and wind speed (WS), were classified into two aspects, (1) Photochemical Reaction Condition (PRC = T_2 × SW) and (2) Physical Dispersion Capacity (PDC = WS). In this way, a Meteorology Synthetic Index (MSI = PRC/PDC) was developed for the quantification of meteorology-induced ground-level O_3 pollution. The positive linear relationship between the 90th percentile of MDA8 (maximum daily 8-h average) O_3 concentration and MSI determined that the contribution of meteorological changes to ground-level O_{-3} varied on a latitudinal gradient, decreasing from ~40% in southern China to 10%–20% in northern China. Favorable photochemical reaction conditions were more important for ground-level O_3 pollution. This study proposes a universally applicable index for fast diagnosis of meteorological roles in ground-level O_3 variability, which enables the assessment of the observed effects of precursor emissions reductions that can be used for designing future control policies.

Key words: ground-level ozone, meteorology synthetic index, photochemical reaction condition, physical dispersion capacity

Citation: Chen, W. H., and Coauthors, 2022: A new index developed for fast diagnosis of meteorological roles in ground-level ozone variations. *Adv. Atmos. Sci.*, **39**(3), 403–414, https://doi.org/10.1007/s00376-021-1257-x.

Article Highlights:

- A Meteorology Synthetic Index (MSI) was developed for fast diagnosis of meteorological roles in ground-level O_3 variation.
- Meteorological conditions contributed to a 10%–40% increase in ground-level O_3 in China for the period 2013–2019.
- The contribution of meteorological parameters to ground-level O_3 decreased from ~40% in southern China to 10%–20% in northern China.

1. Introduction

Ground-level O_3, a secondary pollutant, is formed by sunlight-initiated chemical reactions between nitrogen oxides (NO_x = NO + NO_2) and volatile organic compounds (VOCs). O_3 controls the oxidizing capacity of the atmosphere and causes damage to vegetation growth and human health (Seinfeld and Pandis, 1998). Aircraft observations have revealed an increase in tropospheric O_3 across the Northern Hemisphere since the mid-1990s (Gaudel et al., 2020). While ground-based observations indicate that ground-level O_3 has declined in large urban regions across the United States and Europe owing to the effective control of NO_x and VOC emissions since the 1990s (Cooper et al., 2012; Paoletti et al., 2014), the situation is still severe in China. The spread and worsening of ground-level O_3 in most urban areas of China has become one of the top environmental issues in recent years (Lu et al., 2018; Li et al., 2019; Liu and Wang, 2020a, b; Wang et al., 2020). Lu et al. (2020) concluded that MDA8-O_3 levels increased by 2.4 ppb (5.0%) yr^{-1} in China during the warm season (April–September) for the period 2013–19. More importantly, worsening O_3 pollution with a greater frequency of high-concentration events is

* Corresponding author: Xuemei WANG
Email: eciwxm@jnu.edu.cn

predicted to continue due to the combined effects of emission variations and climate change (Wang et al., 2013; Lee et al., 2015; Cao and Yin, 2020).

Precursor emissions and meteorological conditions are the most important factors controlling the levels and trends of ground-level O_3 (Lu and Chang, 2005; Lu et al., 2019a, b). Stringent clean air actions have been implemented in China since 2013, leading to significant decreases in anthropogenic emissions of NO_x with a relative change of –21% from 2013 to 2017, and further abatement is expected, while VOC emissions increased by 2% in 2017 relative to 2013 and have remained stable since 2017 (Zheng et al., 2018; Dang and Liao, 2019; Li et al., 2020). Significant progress has been made in understanding ground-level O_3 formation from precursor emissions under different meteorological conditions (Steiner et al., 2010). Extensive studies have pointed out that anthropogenic emissions are the dominant factor driving the increase in ground-level O_3 (Lu et al., 2018, 2019a; Li et al., 2019, 2020; Liu and Wang, 2020b), while meteorological conditions have also exerted considerable influence on ground-level O_3 variability (Li et al., 2013; Fu and Tian, 2019; Gong and Liao, 2019; Li et al., 2019, 2020; Han et al., 2020; Le et al., 2020; Zhao et al., 2020). In general, higher surface temperatures and stronger solar radiation, coupled with lower relative humidity (RH), collectively linked with lower cloud fraction, favor the chemical production of O_3 (Peterson and Flowers, 1977; Xu et al., 2011; Lee et al., 2014; Coates et al., 2016; Gong and Liao, 2019; Li et al., 2020; Dang et al., 2021), whereas lower wind speed (WS) and planetary boundary layer height (PBLH) are conducive to the accumulation of O_3 (Haman et al., 2014; Wang et al., 2017; Liu and Wang, 2020a), which results in higher O_3 concentrations. The quantification of meteorology-induced ground-level O_3 is of great importance since meteorological variation may mask the trends in O_3 concentration caused by precursor emissions and influence the development of further mitigation policies (Lu and Chang, 2005; Wang et al., 2018; Liu and Wang, 2020a; Ordóñez et al., 2020). Dang et al. (2021) and Li et al. (2020) reported that meteorological change favored MDA8-O_3 increases, with respective contributions of ~40% and 80% in northern and eastern China during 2012–19.

Chemical transport models (CTMs), one of the most widely used methods to quantify the contribution of meteorological variation, can provide a comprehensive evaluation of the effects of meteorology on the temporal variation of ground-level O_3; however, the large consumption of computational resources and high uncertainties in O_3 simulations (e.g., emission inventory, chemical mechanisms) could make the application of CTM inconvenient (Foley et al., 2015; Lu et al., 2019a; Butler et al., 2020; Liu and Wang, 2020b). Statistical models that develop a relationship between O_3 and meteorological parameters represent another approach to quantify the contribution of meteorological variation to O_3 trends (Kovač-Andrić et al., 2009). Among them, multiple linear regression (MLR) is one of the most frequently employed methods for predicting O_3 concentration as a function of meteorological parameters (Zhong et al., 2018; Li et al., 2019, 2020; Yang et al., 2019). MLR models often consider a certain number of meteorological parameters, which could cause an overfitting issue when the model is too complex and produce misleading R (Correlation Coefficient)-squared values, regression coefficients, and p-values that represent noise rather than genuine relationships. It is known that ground-level O_3 formation and evaluation are comprehensively influenced by multiple meteorological parameters, and the processes of each individual meteorological parameter on ground-level O_3 are quite different and could have specific physical implications (Kayes et al., 2019; Li et al., 2020). Although great effort has been devoted to elucidating the complex interaction between ground-level O_3 and meteorological conditions in recent years (Kovač-Andrić et al., 2009; Otero et al., 2018; Yu et al., 2019), a fast and effective method is still urgently needed to better describe and quantify the comprehensive effects of meteorological conditions on ground-level O_3 variation in the face of the worsening O_3 situation, and ultimately to determine the gaps between precursor emissions controls and the desired reductions in peak O_3 levels.

In this study, a Meteorology Synthetic Index (MSI), as a function of surface temperature, solar radiation, and wind speed, was developed for fast diagnosis of meteorological roles in ground-level O_3 formation by integrating ground-based measurements and outputs from a mesoscale numerical weather prediction model (Weather Research and Forecasting model, WRF). The index was further applied to evaluate the meteorology-induced ground-level O_3 changes in China during 2013–19 based on the linear relationship established between the meteorology index and O_3. The meteorology index established in this study not only enables a fast method for quantitative assessment of meteorological influences on ground-level O_3 variability but also provides meteorological insight into the formation and evaluation of ground-level O_3 pollution through chemical and physical aspects. This study facilitates an in-depth understanding of meteorology-induced ground-level O_3 variations and urges a re-examination of the significance of meteorology for the responses of O_3 pollution to precursor emissions in the face of climate change.

The remainder of this paper is organized as follows. Section 2 describes the materials and methods used in this study, section 3 presents the status of ground-level ozone, section 4 quantifies the contribution of meteorological conditions to annual ozone enhancement and section 5 provides a brief conclusion and discussion.

2. Materials and methods

2.1. *Data*

2.1.1. *Observed ground-level ozone data*

Hourly observational ground-level O_3 concentration

data for 2013–19 were obtained from the public website of the China Ministry of Ecology and Environment (MEE) (http://www.mee.gov.cn/). Five key regions that have been experiencing the most serious O_3 pollution in China were targeted in this study (Fig. 1). These five regions were categorized as follows: Beijing-Tianjin-Heibei (BTH, 55 cities, 280 sites), Fenwei Plain city cluster (FWP, 11 cities, 59 sites), Yangtze River Delta (YRD, 41 cities, 243 sites), Sichuan Basin (SCB, 16 cities, 68 sites), and Pearl River Delta (PRD, 9 cities, 56 sites). A total of 568 air quality stations were used in this study.

Data processing followed the strict criteria presented in the work of Lu et al. (2020) and Song et al. (2017). In brief, 1-h O_3 concentration at each site in a specific city was averaged first, and then the values in certain cities in a specific region were averaged to represent regional results. O_3 exceedance was defined as the number of days with MDA8-O_3 exceeding the Chinese Grade-II (urban/industrial and surrounding rural areas) National Air Quality Standard (160 μg m^{-3}) (General Administration of Quality Supervision, Inspection and Quarantine of the People's Republic of China, and Standardization Administration, 2016).

2.1.2. *Observed meteorological data*

Observational daily meteorological data, including 2-meter temperature (T_2), wind speed (WS), relative humidity (RH), and pressure for China from 2013 to 2019 were obtained from the National Meteorological Information Center, China Meteorological Administration (CMA) (http://data.cma.cn/). A total of 103 meteorological stations were used in this study (Fig. 1). It is worth noting that only 10 stations were available for observed solar radiation, which located in different provinces across all of China (Fig. 1). Hourly observational solar radiation (SW) and planetary boundary layer height (PBLH) obtained by Jinan University (JNU, 23.015°N, 113.419°E), Guangzhou, China, from October 2019 to May 2020 were also collected in this study.

2.1.3. *Simulated meteorological data*

Owing to the small amount (only 10 sites) of available contemporaneously measured public data for SW, T_2, and WS in China, simulated meteorological results from numerical models were applied in this work. Simulated daily meteorological data at a horizontal resolution of 27 km × 27 km, including T_2, SW, WS, RH, PBLH, pressure, and precipitation for the period 2013–19, were obtained from the WRF model (Grell et al., 2005). Detailed information for the WRF model configuration is provided in our previous study (Ma et al., 2020). The WRF-derived data can characterize the meteorological properties of China at a finer scale better than the coarse-resolution reanalysis data that have been used in previous studies, such as the 1° × 1° National Centers for Environmental Prediction (NCEP) Final (FNL) reanalysis data (Han et al., 2020), the 1° × 1° ERA-Interim reana-

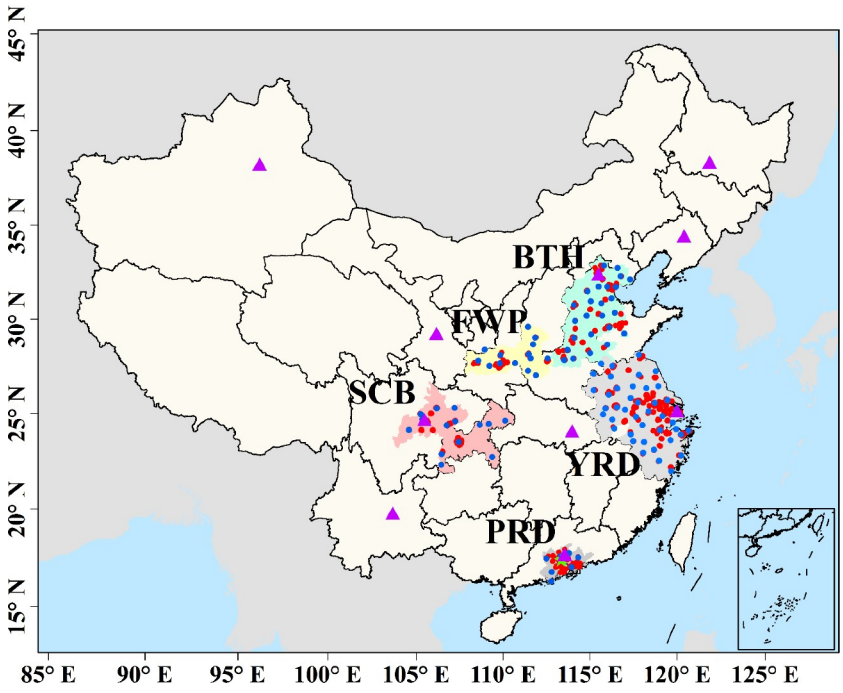

Fig. 1. Map of study regions and locations of O_3 (red dots) and meteorology (blue dots) monitoring sites in China. The Jinan University (JNU) and Panyu Middle School (PYMS) sites are indicated by green stars. The 10 observed solar radiation sites are indicated with rose triangles. Key regions in jade, olive, medium blue, pink, and gray represent the Beijing-Tianjin-Heibei (BTH), Fenwei Plain city cluster (FWP), Yangtze River Delta (YRD), Sichuan Basin (SCB), and Pearl River Delta (PRD) regions, respectively.

lysis dataset (Cao and Yin, 2020; Mousavinezhad et al., 2021), and the 0.5° (lat) × 0.625° (lon) NASA Modern-Era Retrospective Analysis for Research and Applications, Version 2 (MERRA-2) product (Li et al., 2019, 2020).

2.2. *Development of the meteorology index*

Apart from precursor emissions, the formation of ground-level O_3 is controlled by multiple meteorological parameters through different physical and chemical processes. Previous studies have revealed that T_2 and SW are the critical factors determining O_3 photochemical reactions since they respectively affect the reaction kinetic rates and drive photolysis to trigger chain reactions, irrespective of season or region (Peterson and Flowers, 1977; Hsu, 2007; Im et al., 2011; Xu et al., 2011; Jing et al., 2014; Lee et al., 2014; Pusede et al., 2015; Coates et al., 2016; Wang et al., 2017; Ding et al., 2019; Yang et al., 2021), while the WS and PBLH control the horizontal dilution and vertical mixing of O_3 and its precursors, respectively (Haman et al., 2014; Wang et al., 2017; Liu and Wang, 2020a). In addition, RH, cloud fraction, precipitation, and wind direction also show impacts on ground-level O_3 (Li et al., 2019, 2020; Han et al., 2020; Dang et al., 2021).

Previous studies have also pointed out that high temperatures, strong solar radiation, weak wind, and high pressure are usually followed by O_3 episodes, although the meteorological factors affecting ozone formation and accumulation depend on the region (Mousavinezhad et al., 2021). The meteorological factors interact with each other and are not independent variables: temperature can be a surrogate for pressure; solar radiation can be a surrogate for other factors such as relative humidity, cloud fraction, and precipitation; and wind speed can be a surrogate for PBLH (Gong and Liao, 2019). Therefore, T_2, SW, and WS were selected as the most important meteorological parameters impacting ground-level O_3 concentration. PBLH should not be a strong predictor for atmospheric pollutants (e.g., $PM_{2.5}$, O_3) (Banta et al., 2011; Su et al., 2018) since the relationship between PBLH and atmospheric pollutants is quite complex and is believed to be nonlinear (Wang et al., 2018; Dong et al., 2020); for example, Wang et al. (2020) demonstrated that variation in PBLH was not the driving factor that led to the increase in ground-level O_3 over China from 2013 to 2017. As an example, observed data from JNU revealed that MDA8-O_3 was positively and significantly correlated with daily T_2 [Pearson correlation coefficient (R) = 0.37, p-value (P) < 0.01] and daily SW (r = 0.56, P < 0.01), and negatively associated with daily WS (r = –0.28, P < 0.01) during the monitored period (Fig. S1 in the Electronic Supplementary Material, ESM), while it showed no significant correlation with PBLH and RH.

The meteorological parameters selected above were classified into two terms, one defined as Photochemical Reaction Conditions (PRC), which is a function of T_2 and SW, to indicate the effect of meteorological conditions on the photochemical production of O_3. Observed data from JNU showed that MDA8-O_3 has a stronger positive correlation with PRC (R = 0.82. P < 0.01) than that of T_2 and SW. Physical Dispersion Capacity (PDC), represented by WS, is defined to characterize the capability of O_3 dispersion. With higher values of PRC and PDC, meteorological conditions are more conducive to photochemical reactions and dynamic ventilation of ground-level O_3, respectively. Based on the linear relationships between MDA8-O_3, PRC, and PDC, and the MSI, a function of PRC and PDC, is here introduced as a new indicator to comprehensively describe the effect of meteorological variability on ground-level O_3 concentration. MSI can be described as follows:

$$\mathrm{MSI} = \frac{\mathrm{PRC}}{\mathrm{PDC}} = \frac{T_2 \times \mathrm{SW}}{\mathrm{WS}}. \quad (1)$$

The meteorological parameters used in Eq. (1) were first nondimensionalized to make them comparable. In contrast to mean normalization—one of the methods for dimensionless parameters that use the mean value of a specific vector as the denominator, which cannot characterize the geographic and seasonal differences in meteorology—a specific value is used as the denominator in this study to characterize the geographic and seasonal differences in meteorology. It is worth noting that the specific value of the denominator neither affects the trends of meteorological parameters nor the relative contribution of meteorology to O_3 variation, although the magnitude of the meteorological factors will be different. Therefore, the specific values were set to be 25°C, 300 W m^{-2}, and 3 m s^{-1} for T_2, SW, and WS, respectively, which are the average values in southern China. Higher values of MSI denote favorable meteorological conditions for the formation of O_3 and result in higher ground-level O_3 concentrations. Days with rain events were removed from the analysis because O_3 concentration is relatively lower during a rain event, and precipitation is an obvious meteorological parameter affecting O_3 concentration (Wang et al., 2018).

2.3. *Evaluation of the meteorology index*

The limited hourly observational data obtained from JNU were used to evaluate the performance of MSI in predicting ground-level O_3 concentration. Hourly O_3 concentration data were derived from the nearest (straight line distance is ~10 km) air quality monitoring site at Panyu Middle School (PYMS, 22.948°N, 113.352°E). In addition, observed meteorological parameters at the 10 sites across all of China were also used to evaluate MSI performance. Observed O_3 concentration at these 10 meteorological sites was derived from the nearest air quality monitoring site because O_3 observation stations are not collocated with meteorology observation stations. To evaluate MSI, the correlation coefficients between MDA8-O_3 concentration and individual meteorological parameters (i.e., T_2, SW, PBLH, WS, and RH), MSI, and other possible configurations of MSI at JNU and the 10 sites were calculated, as illustrated in Figs. 2 and 3. The other possible configurations of MSI include: $T_2 \times \mathrm{SW}$, $T_2 \times \mathrm{SW/RH}$, $T_2 \times \mathrm{SW/(WS \times RH)}$, and $T_2 \times \mathrm{SW/(WS \times RH \times PBLH)}$.

At JNU sites (Fig. 2), the correlation coefficient between MDA8-O_3 and MSI with a value of 0.77 and 0.94 during the whole period and polluted period, respectively, was higher than that between MDA8-O_3 and the individual meteorological parameters; meanwhile, the corresponding coefficient for MSI was also higher than that of other configurations of MSI, except for $T_2 \times SW/(WS \times RH)$. In terms of the 10 stations (Fig. 3), the corresponding coefficients for MSI were again higher than that of individual meteorological parameters, except for T_2, which was comparable with MSI. As compared with other configurations of MSI, 6 out of 10 sites showed the highest coefficients for MSI, whereas only Kunming presented the lowest coefficient for MSI. The coefficient for MSI was comparable with $T_2 \times SW$ in the rest of the three sites. Overall, the results at JNU and the 10 stations suggested that the MSI developed in this study can better represent the meteorological influences compared with single meteorological parameters and other configurations of MSI.

2.4. *Quantitative diagnosis of meteorology-induced ozone variation*

The regional-scale MSI was calculated through simulated historical meteorological parameters from the WRF model during 2013–19. The simulated data were first evaluated by comparison with ground-based measurements (Fig. S2 in the ESM). The statistical results for meteorological parameters are presented in Table S1 in the ESM. Figure S2 illustrates that most data points fall around the 1:1 line for T_2, and most are within the twofold range for WS. The root mean square error (RMSE) was 0.66°C–2.33°C for T_2 and 1.20–2.66 m s^{-1} for WS. Overall, modeled meteorology trends closely resembled the observed trends, with a R of ~0.99 for T_2 and 0.31–0.74 for WS ($P < 0.01$). Solar radiation data collected from JNU and 10 sites over China were also used to evaluate the simulation results (Fig. S3 in the ESM). While the WRF model underestimated SW at JNU from October 2019 to May 2020 with an RMSE of 145 W m^{-2}, it captured the tendency well, with an R of 0.5 ($P < 0.05$). Simulated SW over China agreed well with the observations for the period 2013–19, with an RMSE and R of 18 W m^{-2} and 0.85 ($P < 0.01$), respectively. Overall, the WRF model reasonably captured the magnitude and spatiotemporal distribution of meteorological parameters in China during 2013–19.

To quantify the meteorology-induced ground-level O_3 variation, a linear regression model between the monthly 90th percentile MDA8-O_3 and MSI was established and further applied to quantify the contribution of meteorology to ground-level O_3 variability over China for historical (2013–19) periods. The fitting parameters for the linear regression model are listed in Table S2 and shown in Fig. S4 in the ESM. The determination coefficient (R^2) represents the percentage of the variance in the observed data explained by the model. R^2 ranged between 0.47 and 0.82 in the regression ($P < 0.01$), indicating that the meteorological variables selected in this study can explain 47%–82% of the variance of the 90th percentile MDA8-O_3 for the period 2013–2019. The discrepancy between the meteorology-induced 90th percentile MDA8-O_3 variation and the observed changes in the 90th percentile MDA8-O_3 might be attributed to contributions from other meteorological parameters not considered in this study (e.g., RH, pressure, cloud fraction), precursor emission variations, $PM_{2.5}$ level, etc. (Zhong et al., 2018; Li et al., 2019; Yang et al., 2019).

3. Status of ground-level ozone

The 12-month moving average for the 2nd, 50th, and 90th percentiles of MDA8-O_3 showed significant positive trends ($P < 0.05$) in China for the entire period (Fig. 4a), with a rate of 0.22, 0.28, and 0.32 μg m^{-3} $month^{-1}$, respectively. The growth rate for MDA8-O_3 increased with the percentiles, indicating that heavy O_3 pollution has been getting worse across all of China. Accordingly, significant enhancement in the magnitude and frequency of high O_3 events was

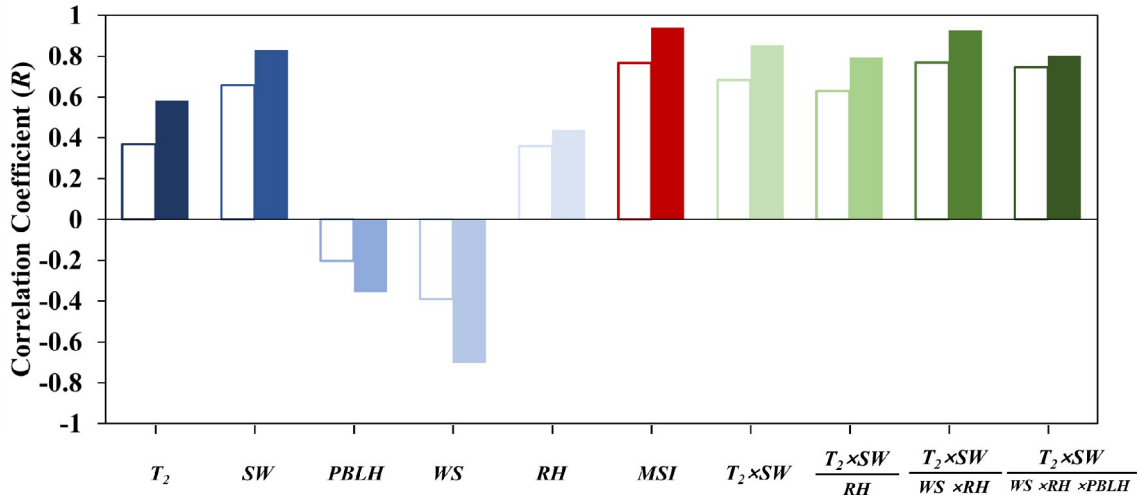

Fig. 2. Correlation coefficients for MDA8-O_3 concentration and each meteorological factor at the JNU site during the whole period (hollow bars) and during a heavy O_3 pollution period (solid bars).

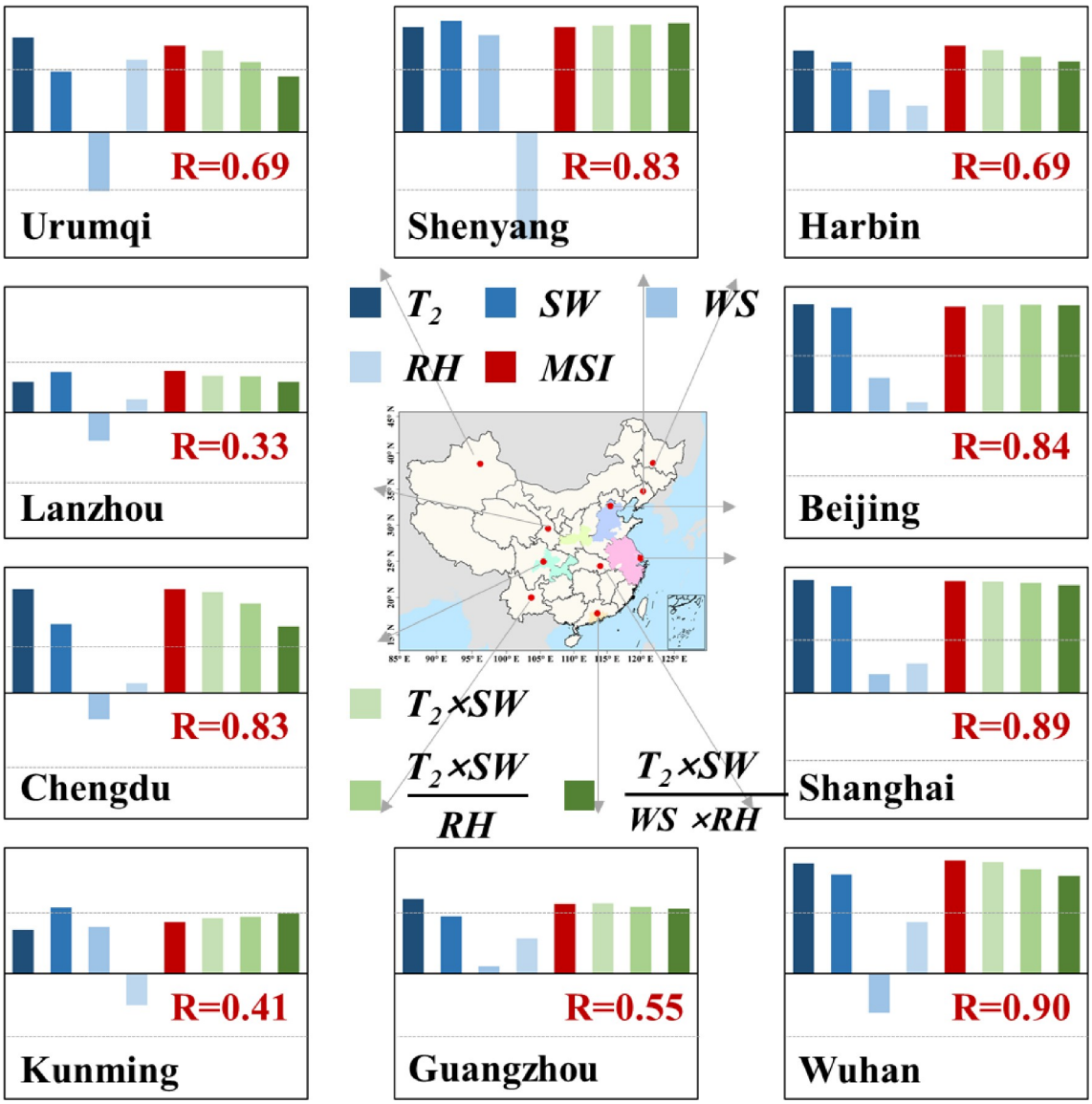

Fig. 3. Correlation coefficients for monthly MDA8-O_3 concentration and each meteorological factor at the 10 sites across China during 2013–19. The correlation coefficients between MDA8 -O_3 and MSI at the 95% confidence level are shown in each plot. The *Y*-axis in each plot ranges from –1 to 1.

observed (Fig. S5 in the ESM), with the annual average O_3 exceedance rapidly increasing from 8 days (2%) in 2013 to 36 days (10%) in 2019 at the rate of 5 d yr^{-1} ($P < 0.05$) over China. To be more specific, relatively higher growth rates occurred in the BTH and FWP regions, with values ranging between 0.35 and 0.61 μg m^{-3} $month^{-1}$, followed by the YRD and SCB regions with a value of 0.13–0.37 μg m^{-3} $month^{-1}$, while MDA8-O_3 climbed with fluctuation in the PRD region at a rate of 0.16–0.29 μg m^{-3} $month^{-1}$. The O_3 exceedance was the most serious in the BTH region, where it reached up to 40–60 days (10%–15%) since 2017 with a growth rate of 8 d yr^{-1}, followed by the FWP, YRD, and PRD regions, with a value of 20–30 days (10%) since 2017 and a growth rate of ~5 d yr^{-1}; however, SCB had relatively slight exceedance (< 10 days), with a growth rate of ~2 d yr^{-1}.

It is worth noting that there was a rightward shift in the histogram of daily MDA8-O_3 across the five key regions relative to the periods of 2013–16 and 2017–19 (Fig. 5), and the corresponding values for peak frequency of daily MDA8-O_3 increased by about 20 μg m^{-3} during these two periods, suggesting that a wide range of worsening O_3 pollution has been particularly prominent since 2017 across all of China. In addition, the frequency of high O_3 events with daily MDA8-O_3 above 160 μg m^{-3} has grown by 3.6% from 2013–16 to 2017–19 on average, varying between 1.9% in the SCB region and 9.9% in the BTH region. More importantly, an elevated frequency of extremely high O_3 events (MDA8-O_3 > 200 μg m^{-3}) was also detected, with a value of +1.2% on average, and the situation was the most serious in the BTH region with a corresponding value of +4.7%. From the perspective of anthropogenic emissions, lower O_3 titra-

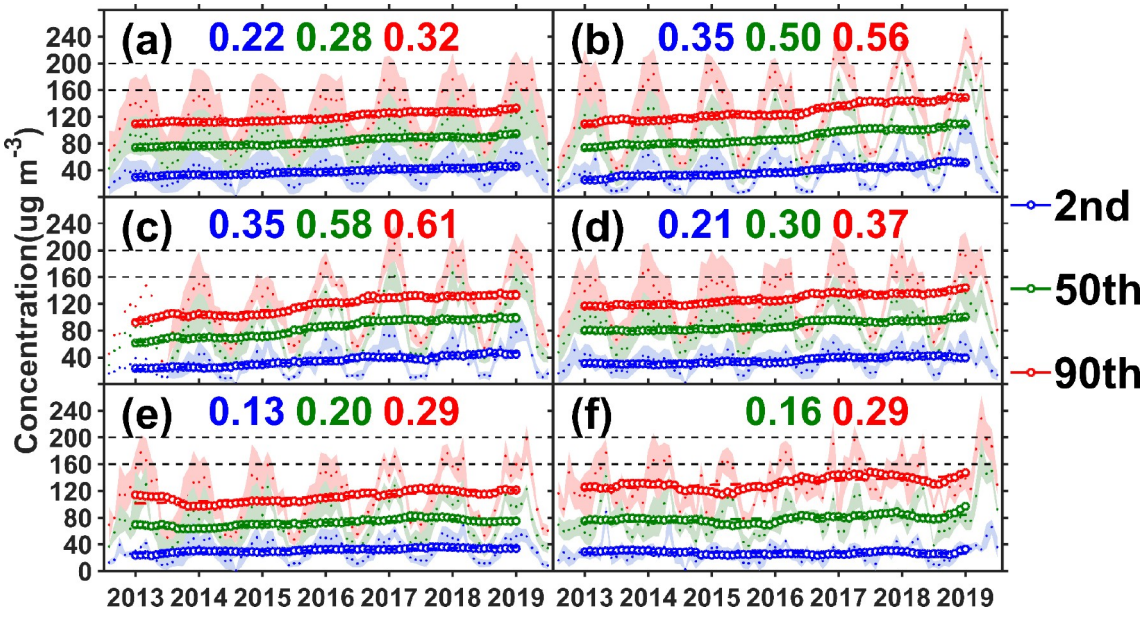

Fig. 4. Trends of monthly and 12-month moving average 2nd, 50th, and 90th percentile values of MDA8-O_3 concentration. (a) China; (b) BTH; (c) FWP; (d) YRD; (e) SCB; (f) PRD. The shaded areas represent the corresponding standard deviations. For reference, 160 and 200 μg m^{-3} concentrations are indicated by black dashed lines, which correspond to the Chinese Grade-II and Grade-I National Air Quality Standards, respectively. The slopes for the linear regression at the 95% confidence level are shown in each plot.

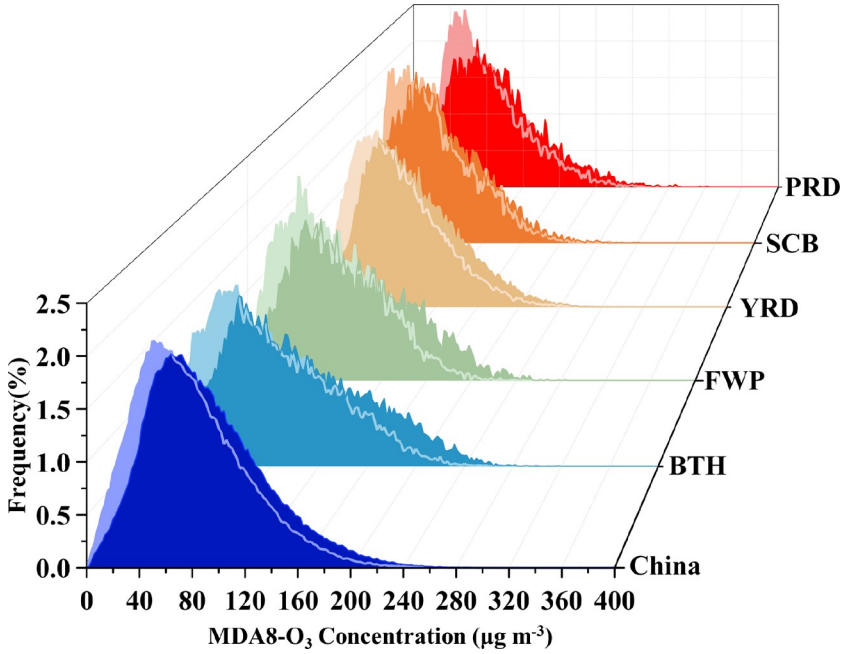

Fig. 5. Histograms of daily MDA8-O_3 in the study regions for the period 2013–2016 (light-colored areas) and 2017–2019 (dark-colored areas), respectively.

tion by NO resulting from the continuous reduction in NO_x emissions could have resulted in the enhancement of ground-level O_3 since 2017 under conditions where VOC emissions remained stable after 2017 (Zheng et al., 2018; Dang and Liao, 2019). Meteorological conditions are likely to have been another important factor contributing to the more severe O_3 pollution during 2017–19 compared with that during 2013–17 (Li et al., 2020).

4. Meteorological conditions contributing to annual ozone enhancement

Long-term trends of the meteorology indices presented in Fig. S6 reveal that statistically significant upward trends

(0.07%–0.29% month^{-1}, $P < 0.05$) and downward trends (–0.17%–0.04% month^{-1}, $P < 0.05$) were observed for PRC and PDC ($P < 0.05$) from 2013 through 2019, respectively, except for PDC in the BTH region, where WS remained stable. Consequently, significant positive changes in MSI have been noted in the study regions (0.15%–0.44% month^{-1}, $P < 0.05$). This illustrative analysis suggests that meteorological conditions with stronger photochemical reaction conditions and weaker physical dispersion conditions could have progressively increased ground-level O_3 concentrations in recent years.

Figure 6 summarizes the variation of 90th percentile MDA8-O_3 (hereafter referred to as Δ90th MDA8-O_3) for the period 2013–19 caused by meteorological changes. Overall, Δ90th MDA8-O_3 caused by meteorological changes was estimated to be 1.4 ± 0.4 μg m^{-3} yr^{-1}, accounting for 28% of observed Δ90th MDA8-O_3 over China. Interestingly, the contribution of meteorological changes to Δ90th MDA8-O_3 varied on a latitudinal gradient, decreasing from ~40% in southern China (YRD, SCB, and PRD regions) to ~20% in the FWP region and ~10% in the BTH region. Upon further analysis, a region-specific difference in the relative importance of PRC and PDC to MSI was detected across China. Among them, the weakening of wind speed (PDC) played a more important role in the increment of MSI in the SCB region, where the blocking effects of the terrain can lead to stagnant conditions and thermal inversion (Wang et al., 2018; Miao et al., 2019), while the influences of PRC and PDC were comparable in the FWP and YRD regions. The intensification of ambient conditions favoring photochemical reactions, with increasing PRC, was more crucial than that of physical dispersion conditions for the growth of MSI in the PRD and BTH regions. The results demonstrate that meteorology exerted a larger influence on ground-level O_3 pollution in southern China and less influence in northern China. This is because, on the one hand, the variation in MSI was much lower in northern China (0.0011 per month in the BTH) than in southern China (0.0033 per month in the PRD), as shown in Fig. S6c; on the other hand, the amount and variation of anthropogenic emissions were more obvious in northern China than in southern China (Ding et al., 2019; Liu and Wang, 2020b), resulting in the relatively lower contribution of meteorology in northern China. Previous studies have also proven that anthropogenic emission vari-

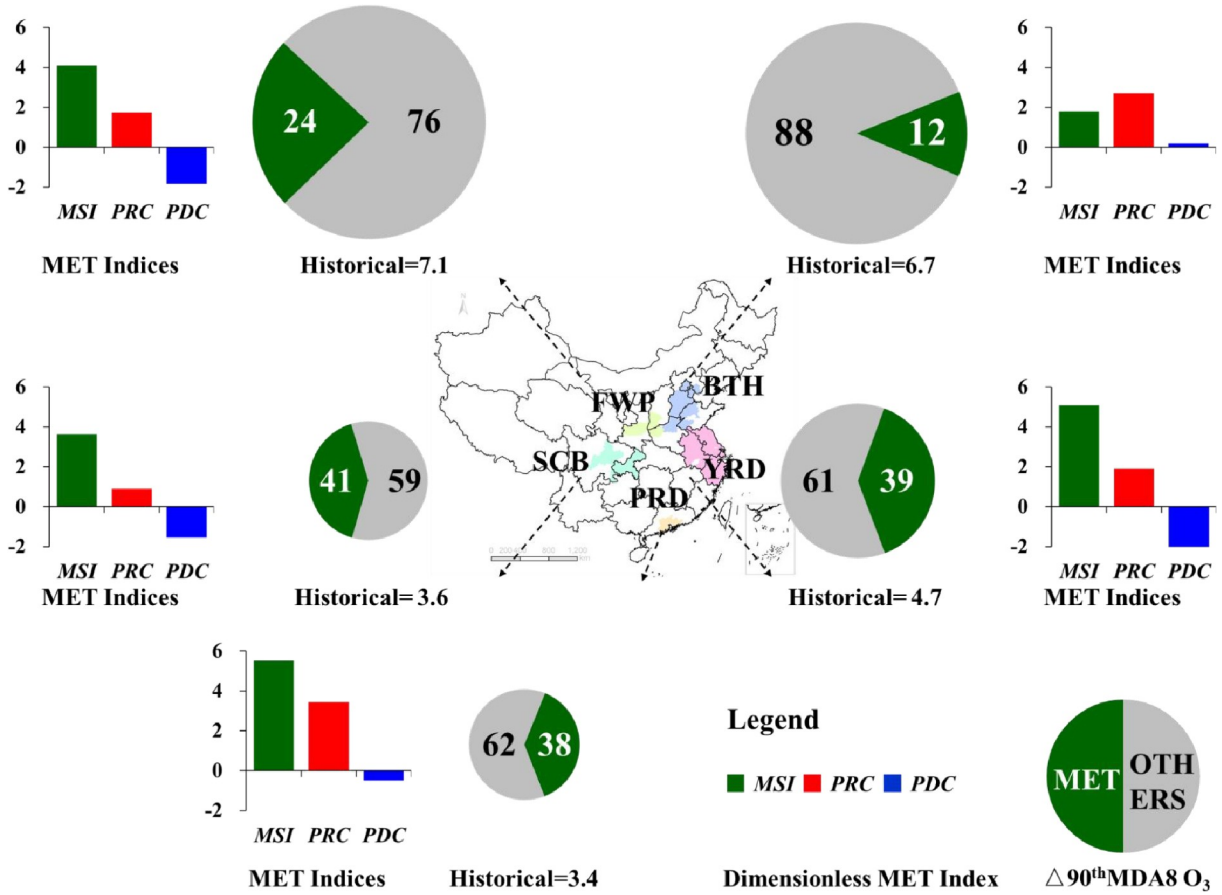

Fig. 6. Variation of 90th percentile MDA8-O_3 (Δ90th MDA8-O_3) attributed to meteorology (MET) and other factors (OTHERS) in the study regions across China during 2013–2019. Pies with dark green and grey represent the relative contribution (%) of MET and OTHERS to the Δ90th MDA8-O_3 concentration. Variation rates (μg m^{-3} yr^{-1}) of Δ90th MDA8-O_3 are inserted below the pies and characterized by the size of the pies. Bars indicate the variation rates (% yr^{-1}) of the normalized meteorological indices.

ation showed a more predominant role in ground-level O_3 in northern China (Li et al., 2020; Liu and Wang, 2020a, b; Mousavinezhad et al., 2021).

The contribution of meteorological variation estimated in this study was compared with results from previous studies that used chemical transport models or statistical methods, as is summarized in Table S3 in the ESM. In general, the magnitude and direction of meteorology-induced O_3 variation were quite different, depending on the study region and methods used. Most studies concluded that meteorological conditions favored the incremental increase in O_3 concentration in China, except for Ma et al. (2016) and Li et al. (2020), who found that meteorological variation led to a decrease in O_3 in northern China and the SCB region. In contrast, Ding et al. (2019) and Lou et al. (2015) pointed out that the negative effect of changes in emissions was offset by meteorological variation, and the O_3 incremental changes were caused mainly by changes in meteorological conditions, with a contribution higher than 100%, rather than by emissions in China based on the CMAQ and GEOS-Chem models, respectively. Specifically, the contribution of meteorological factors (10%–20%) in northern China estimated in this study was relatively lower than that calculated in previous studies (32%–80%). The corresponding value was ~40% in eastern China, which was comparable to or relatively lower than that derived from previous studies (43%–84%). In southern China, the contribution was ~40%, which was comparable with previous studies in the range of 15%–92%. Overall, the meteorological contribution was underestimated in this study compared with some previous studies since this study included only three dominant meteorological factors while previous studies considered many more meteorological parameters.

5. Conclusion and discussion

Severe ground-level O_3 pollution with significant enhancement in the magnitude and frequency of high O_3 events was observed in China from 2013 to 2019. In this study, the most important meteorological parameters, including T_2, SW, and WS, were selected and classified into two terms, defined as PRC = T_2 × SW and PDC = WS, to separate the meteorological influences on O_3 through different aspects. Then a MSI was developed as a function of PRC and PDC to better outline and quantify the comprehensive impacts of meteorological conditions on ground-level O_3 variability. The results demonstrated that the change in meteorology-induced 90th percentile MDA8-O_3 was estimated to be 1.4 ± 0.4 μg m^{-3} yr^{-1} on average. Adverse meteorology, with stronger photochemical reaction conditions and weaker physical dispersion capacity, accounted for 10%–40% of the increase in 90th percentile MDA8-O_3, with a higher (lower) contribution in southern (northern) China.

This study is subject to high uncertainty. First, only three meteorological parameters were considered, which cannot fully represent the influences of meteorological conditions since O_3 is controlled by multiple meteorological parameters, such as PBLH, RH, cloud fraction, pressure (Li et al., 2019, 2020; Zhao et al., 2021). Second, ground-level O_3 is affected not only by local meteorology, but also by large-scale weather circulation conditions (Gong and Liao, 2019; Liu et al., 2019; Liao et al., 2021), such as typhoons (Wei et al., 2016), the East Asian monsoon (Zhou et al., 2013; Yang et al., 2014), the western Pacific subtropical high (Liao et al., 2017; Zhao and Wang, 2017), the mei-yu front (Han et al., 2020), and El Niño-Southern Oscillation (ENSO) (Sekiya and Sudo, 2014). Third, this study did not consider chemical reactions that also affect ground-level O_3 since precursor emissions are also impacted by meteorological conditions (Lu et al., 2019b; Liu and Wang, 2020b; Dang et al., 2021). Although high uncertainty exists, the meteorology index established in this study not only enables fast diagnosis of meteorological roles in ground-level O_3 formation but also provides insight into meteorological influences on the formation and evaluation of ground-level O_3 pollution through its chemical and physical aspects. Results in this study signify that precursor emission reductions will need to be more stringent to counteract the adverse effects of long-term meteorological variation on ground-level O_3 pollution in the face of climate change.

Acknowledgements. This study was supported by the National Key Research and Development Plan (Grant No. 2017YFC0210105), the second Tibetan Plateau Scientific Expedition and Research Program (Grant No. 2019QZKK0604), the National Natural Science Foundation of China (Grant Nos. 41905086, 41905107, 42077205, and 41425020), the Special Fund Project for Science and Technology Innovation Strategy of Guangdong Province (Grant No. 2019B121205004), the China Postdoctoral Science Foundation (Grant No. 2020M683174), the AirQuip (High-resolution Air Quality Information for Policy) Project funded by the Research Council of Norway, the Collaborative Innovation Center of Climate Change, Jiangsu Province, China, and the high-performance computing platform of Jinan University.

Electronic supplementary material: Supplementary material is available in the online version of this article at https://doi.org/10.1007/s00376-021-1257-y.

REFERENCES

Banta, R. M., and Coauthors, 2011: Dependence of daily peak O_3 concentrations near Houston, Texas on environmental factors: Wind speed, temperature, and boundary-layer depth. *Atmos. Environ.*, **45**, 162–173, https://doi.org/10.1016/j.atmosenv.2010.09.030.

Butler, T., A. Lupascu, and A. Nalam, 2020: Attribution of ground-level ozone to anthropogenic and natural sources of nitrogen oxides and reactive carbon in a global chemical transport model. *Atmospheric Chemistry and Physics*, **20**, 10 707–10 731, https://doi.org/10.5194/acp-20-10707-2020.

Cao, B. F., and Z. C. Yin, 2020: Future atmospheric circulations benefit ozone pollution control in Beijing-Tianjin-Hebei with global warming. *Science of the Total Environment*,

743, 140645, https://doi.org/10.1016/j.scitotenv.2020.140645.

Coates, J., K. A. Mar, N. Ojha, and T. M. Butler, 2016: The influence of temperature on ozone production under varying NO_x conditions–a modelling study. *Atmospheric Chemistry and Physics*, **16**, 11 601–11 615, https://doi.org/10.5194/acp-16-11601-2016.

Cooper, O. R., R. S. Gao, D. Tarasick, T. Leblanc, and C. Sweeney, 2012: Long-term ozone trends at rural ozone monitoring sites across the United States, 1990–2010. *J. Geophys. Res.*, **117**, D22307, https://doi.org/10.1029/2012JD018261.

Dang, R. J., and H. Liao, 2019: Radiative forcing and health impact of aerosols and ozone in China as the consequence of clean air actions over 2012–2017. *Geophys. Res. Lett.*, **46**, 12 511–12 519, https://doi.org/10.1029/2019GL084605.

Dang, R. J., H. Liao, and Y. Fu, 2021: Quantifying the anthropogenic and meteorological influences on summertime surface ozone in China over 2012-2017. *Science of the Total Environment*, **754**, 142394, https://doi.org/10.1016/j.scitotenv.2020.142394.

Ding, D., J. Xing, S. X. Wang, X. Chang, and J. M. Hao, 2019: Impacts of emissions and meteorological changes on China's ozone pollution in the warm seasons of 2013 and 2017. *Frontiers of Environmental Science & Engineering*, **13**, 76, https://doi.org/10.1007/s11783-019-1160-1.

Dong, Y. M., J. Li, J. P. Guo, Z. J. Jiang, Y. Q. Chu, L. Chang, Y. Yang, and H. Liao, 2020: The impact of synoptic patterns on summertime ozone pollution in the North China Plain. *Science of the Total Environment*, **735**, 139559, https://doi.org/10.1016/j.scitotenv.2020.139559.

Foley, K. M., C. Hogrefe, G. Pouliot, N. Possiel, S. J. Roselle, H. Simon, and B. Timin, 2015: Dynamic evaluation of CMAQ part I: Separating the effects of changing emissions and changing meteorology on ozone levels between 2002 and 2005 in the eastern US. *Atmos. Environ.*, **103**, 247–255, https://doi.org/10.1016/j.atmosenv.2014.12.038.

Fu, T. M., and H. Tian, 2019: Climate change penalty to ozone air quality: Review of current understandings and knowledge gaps. *Current Pollution Reports*, **5**, 159–171, https://doi.org/10.1007/s40726-019-00115-6.

Gaudel, A., and Coauthors, 2020: Aircraft observations since the 1990s reveal increases of tropospheric ozone at multiple locations across the Northern Hemisphere. *Science Advances*, **6**, eaba8272, https://doi.org/10.1126/sciadv.aba8272.

Gong, C., and H. Liao, 2019: A typical weather pattern for ozone pollution events in North China. *Atmospheric Chemistry and Physics*, **19**, 13 725–13 740, https://doi.org/10.5194/acp-19-13725-2019.

Grell, G. A., S. E. Peckham, R. Schmitz, S. A. McKeen, G. Frost, W. C. Skamarock, and B. Eder, 2005: Fully coupled "online" chemistry within the WRF model. *Atmos. Environ.*, **39**, 6957–6975, https://doi.org/10.1016/j.atmosenv.2005.04.027.

Haman, C. L., E. Couzo, J. H. Flynn, W. Vizuete, B. Heffron, and B. L. Lefer, 2014: Relationship between boundary layer heights and growth rates with ground-level ozone in Houston, Texas. *J. Geophys. Res.*, **119**, 6230–6245, https://doi.org/10.1002/2013JD020473.

Han, H., J. Liu, L. Shu, T. J. Wang, and H. L. Yuan, 2020: Local and synoptic meteorological influences on daily variability in summertime surface ozone in eastern China. *Atmospheric Chemistry and Physics*, **20**, 203–222, https://doi.org/10.5194/acp-20-203-2020.

Hsu, K.-J., 2007: Relationships between ten-year trends of tropospheric ozone and temperature over Taiwan. *Science of the Total Environment*, **374**, 135–142, https://doi.org/10.1016/j.scitotenv.2007.01.003.

Im, U., and Coauthors, 2011: The impact of temperature changes on summer time ozone and its precursors in the eastern Mediterranean. *Atmospheric Chemistry and Physics*, **11**, 3847–3864, https://doi.org/10.5194/acp-11-3847-2011.

Jing, P., Z. F. Lu, J. Xing, D. G. Streets, Q. Tan, T. O'Brien, and J. Kamberos, 2014: Response of the summertime ground-level ozone trend in the Chicago area to emission controls and temperature changes, 2005–2013. *Atmos. Environ.*, **99**, 630–640, https://doi.org/10.1016/j.atmosenv.2014.10.035.

Kayes, I., S. A. Shahriar, K. Hasan, M. Akhter, M. M. Kabir, and M. A. Salam, 2019: The relationships between meteorological parameters and air pollutants in an urban environment. *Global Journal of Environmental Science and Management*, **5**, 265–278, https://doi.org/10.22034/gjesm.2019.03.01.

Kovač-Andrić, E., J. Brana, and V. Gvozdić, 2009: Impact of meteorological factors on ozone concentrations modelled by time series analysis and multivariate statistical methods. *Ecological Informatics*, **4**, 117–122, https://doi.org/10.1016/j.ecoinf.2009.01.002.

Le, T. H., Y. Wang, L. Liu, J. N. Yang, Y. L. Yung, G. H. Li, and J. H. Seinfeld, 2020: Unexpected air pollution with marked emission reductions during the COVID-19 outbreak in China. *Science*, **369**, 702–706, https://doi.org/10.1126/science.abb7431.

Lee, J.-B., and Coauthors, 2015: Projections of summertime ozone concentration over East Asia under multiple IPCC SRES emission scenarios. *Atmos. Environ.*, **106**, 335–346, https://doi.org/10.1016/j.atmosenv.2015.02.019.

Lee, Y. C., D. T. Shindell, G. Faluvegi, M. Wenig, Y. F. Lam, Z. Ning, S. Hao, and C. S. Lai, 2014: Increase of ozone concentrations, its temperature sensitivity and the precursor factor in South China. *Tellus B: Chemical and Physical Meteorology*, **66**, 23455, https://doi.org/10.3402/tellusb.v66.23455.

Li, K., D. J. Jacob, H. Liao, L. Shen, Q. Zhang, and K. H. Bates, 2019: Anthropogenic drivers of 2013–2017 trends in summer surface ozone in China. *Proceedings of the National Academy of Sciences of the United States of America*, **116**, 422–427, https://doi.org/10.1073/pnas.1812168116.

Li, K., D. J. Jacob, L. Shen, X. Lu, I. De Smedt, and H. Liao, 2020: Increases in surface ozone pollution in China from 2013 to 2019: Anthropogenic and meteorological influences. *Atmospheric Chemistry and Physics*, **20**, 11 423–11 433, https://doi.org/10.5194/acp-20-11423-2020.

Li, Y., A. K. H. Lau, J. C. H. Fung, J. Y. Zheng, and S. Liu, 2013: Importance of NO_x control for peak ozone reduction in the Pearl River Delta region. *J. Geophys. Res.*, **118**, 9428–9443, https://doi.org/10.1002/jgrd.50659.

Liao, W. H., L. L. Wu, S. Z. Zhou, X. M. Wang, and D. L. Chen, 2021: Impact of synoptic weather types on ground-level ozone concentrations in Guangzhou, China. *Asia-Pacific Journal of Atmospheric Sciences*, **57**, 169–180, https://doi.org/10.1007/s13143-020-00186-2.

Liao, Z. H., M. Gao, J. R. Sun, and S. J. Fan, 2017: The impact of synoptic circulation on air quality and pollution-related human health in the Yangtze River Delta region. *Science of the Total Environment*, **607–608**, 838–846, https://doi.org/10.1016/j.scitotenv.2017.07.031.

Liu, J. D., and Coauthors, 2019: Quantifying the impact of synoptic circulation patterns on ozone variability in northern China from April to October 2013–2017. *Atmospheric Chemistry and Physics*, **19**, 14 477–14 492, https://doi.org/10.5194/acp-19-14477-2019.

Liu, Y. M., and T. Wang, 2020a: Worsening urban ozone pollution in China from 2013 to 2017–Part 1: The complex and varying roles of meteorology. *Atmospheric Chemistry and Physics*, **20**, 6305–6321, https://doi.org/10.5194/acp-20-6305-2020.

Liu, Y. M., and T. Wang, 2020b: Worsening urban ozone pollution in China from 2013 to 2017–Part 2: The effects of emission changes and implications for multi-pollutant control. *Atmospheric Chemistry and Physics*, **20**, 6323–6337, https://doi.org/10.5194/acp-20-6323-2020.

Lou, S. J., H. Liao, Y. Yang, and Q. Mu, 2015: Simulation of the interannual variations of tropospheric ozone over China: Roles of variations in meteorological parameters and anthropogenic emissions. *Atmos. Environ.*, **122**, 839–851, https://doi.org/10.1016/j.atmosenv.2015.08.081.

Lu, H.-C., and T.-S. Chang, 2005: Meteorologically adjusted trends of daily maximum ozone concentrations in Taipei, Taiwan. *Atmos. Environ.*, **39**, 6491–6501, https://doi.org/10.1016/j.atmosenv.2005.06.007.

Lu, X., and Coauthors, 2018: Severe surface ozone pollution in China: A global perspective. *Environmental Science & Technology Letters*, **5**, 487–494, https://doi.org/10.1021/acs.estlett.8b00366.

Lu, X., and Coauthors, 2019a: Exploring 2016-2017 surface ozone pollution over China: Source contributions and meteorological influences. *Atmospheric Chemistry and Physics*, **19**, 8339–8361, https://doi.org/10.5194/acp-19-8339-2019.

Lu, X., L. Zhang, and L. Shen, 2019b: Meteorology and climate influences on tropospheric ozone: A review of natural sources, chemistry, and transport patterns. *Current Pollution Reports*, **5**, 238–260, https://doi.org/10.1007/s40726-019-00118-3.

Lu, X., L. Zhang, X. L. Wang, M. Gao, K. Li, Y. Z. Zhang, X. Yue, and Y. H. Zhang, 2020: Rapid increases in warm-season surface ozone and resulting health impact in China since 2013. *Environmental Science & Technology Letters*, **7**, 240--247, https://doi.org/10.1021/acs.estlett.0c00171.

Ma, M. R., W. H. Chen, S. G. Jia, M. Chang, B. Q. Zhong, and X. M. Wang, 2020: A new method for quantification of regional nitrogen emission-Deposition transmission in China. *Atmos. Environ.*, **227**, 117401, https://doi.org/10.1016/j.atmosenv.2020.117401.

Ma, Z. Q., J. Xu, W. J. Quan, Z. Y. Zhang, W. L. Lin, and X. B. Xu, 2016: Significant increase of surface ozone at a rural site, north of eastern China. *Atmospheric Chemistry and Physics*, **16**, 3969–3977, https://doi.org/10.5194/acp-16-3969-2016.

Miao, Y. C., J. Li, S. G. Miao, H. Z. Che, Y. Q. Wang, X. Y. Zhang, R. Zhu, and S. H. Liu, 2019: Interaction between planetary boundary layer and $PM_{2.5}$ pollution in megacities in China: A review. *Current Pollution Reports*, **5**, 261–271, https://doi.org/10.1007/s40726-019-00124-5.

General Administration of Quality Supervision, Inspection and Quarantine of the People's Republic of China, and Standardization Administration, 2016: Ambient air quality standard: GB 3095–2012. Beijing: China Environmental Science Press. (in Chinese)

Mousavinezhad, S., Y. Choi, A. Pouyaei, M. Ghahremanloo, and D. L. Nelson, 2021: A comprehensive investigation of surface ozone pollution in China, 2015–2019: Separating the contributions from meteorology and precursor emissions. *Atmospheric Research*, **257**, 105599, https://doi.org/10.1016/j.atmosres.2021.105599.

Ordóñez, C., J. M. Garrido-Perez, and R. García-Herrera, 2020: Early spring near-surface ozone in Europe during the COVID-19 shutdown: Meteorological effects outweigh emission changes. *Science of the Total Environment*, **747**, 141322, https://doi.org/10.1016/j.scitotenv.2020.141322.

Otero, N., and Coauthors, 2018: A multi-model comparison of meteorological drivers of surface ozone over Europe. *Atmospheric Chemistry and Physics*, **18**, 12 269–12 288, https://doi.org/10.5194/acp-18-12269-2018.

Paoletti, E., A. De Marco, D. C. S. Beddows, R. M. Harrison, and W. J. Manning, 2014: Ozone levels in European and USA cities are increasing more than at rural sites, while peak values are decreasing. *Environmental Pollution*, **192**, 295–299, https://doi.org/10.1016/j.envpol.2014.04.040.

Peterson, J. T., and E. C. Flowers, 1977: Interactions between air pollution and solar radiation. *Solar Energy*, **19**, 23–32, https://doi.org/10.1016/0038-092X(77)90085-8.

Pusede, S. E., A. L. Steiner, and R. C. Cohen, 2015: Temperature and recent trends in the chemistry of continental surface ozone. *Chemical Reviews*, **115**, 3898–3918, https://doi.org/10.1021/cr5006815.

Seinfeld, J. H., and S. N. Pandis, 1998: *Atmospheric Chemistry and Physics: From Air Pollution to Climate Change*. Wiley-Interscience Publication, 1152 pp.

Sekiya, T., and K. Sudo, 2014: Roles of transport and chemistry processes in global ozone change on interannual and multidecadal time scales. *J. Geophys. Res.*, **119**, 4903–4921, https://doi.org/10.1002/2013JD020838.

Song, C. B., and Coauthors, 2017: Air pollution in China: Status and spatiotemporal variations. *Environmental Pollution*, **227**, 334–347, https://doi.org/10.1016/j.envpol.2017.04.075.

Steiner, A. L., A. J. Davis, S. Sillman, R. C. Owen, A. M. Michalak, and A. M. Fiore, 2010: Observed suppression of ozone formation at extremely high temperatures due to chemical and biophysical feedbacks. *Proceedings of the National Academy of Sciences of the United States of America*, **107**, 19 685–19 690, https://doi.org/10.1073/pnas.1008336107.

Su, T. N., Z. Q. Li, and R. Kahn, 2018: Relationships between the planetary boundary layer height and surface pollutants derived from lidar observations over China: Regional pattern and influencing factors. *Atmospheric Chemistry and Physics*, **18**, 15 921–15 935, https://doi.org/10.5194/acp-18-15921-2018.

Wang, T., L. K. Xue, P. Brimblecombe, Y. F. Lam, L. Li, and L. Zhang, 2017: Ozone pollution in China: A review of concentrations, meteorological influences, chemical precursors, and effects. *Science of the Total Environment*, **575**, 1582–1596, https://doi.org/10.1016/j.scitotenv.2016.10.081.

Wang, X. Y, R. E. Dickinson, L. Y. Su, C. L. Zhou, and K. C. Wang, 2018: $PM_{2.5}$ pollution in China and how it has been exacerbated by terrain and meteorological conditions. *Bull. Amer. Meteor. Soc.*, **99**, 105–119, https://doi.org/10.1175/BAMS-D-16-0301.1.

Wang, Y. H., and Coauthors, 2020: Contrasting trends of $PM_{2.5}$ and surface-ozone concentrations in China from 2013 to 2017. *National Science Review*, **7**, 1331--1339, https://doi.

org/10.1093/nsr/nwaa032.

Wang, Y. X., L. L. Shen, S. L. Wu, L. Mickley, J. W. He, and J. M. Hao, 2013: Sensitivity of surface ozone over China to 2000–2050 global changes of climate and emissions. *Atmos. Environ.*, **75**, 374–382, https://doi.org/10.1016/j.atmosenv.2013.04.045.

Wei, X. L., K.-S. Lam, C. Y. Cao, H. Li, and J. J. He, 2016: Dynamics of the typhoon Haitang related high ozone episode over Hong Kong. *Advances in Meteorology*, **2016**, 6089154, https://doi.org/10.1155/2016/6089154.

Xu, J., and Coauthors, 2011: Measurements of ozone and its precursors in Beijing during summertime: Impact of urban plumes on ozone pollution in downwind rural areas. *Atmospheric Chemistry and Physics*, **11**, 12 241–12 252, https://doi.org/10.5194/acp-11-12241-2011.

Yang, L. F., and Coauthors, 2019: Quantitative impacts of meteorology and precursor emission changes on the long-term trend of ambient ozone over the Pearl River Delta, China, and implications for ozone control strategy. *Atmospheric Chemistry and Physics*, **19**, 12 901–12 916, https://doi.org/10.5194/acp-19-12901-2019.

Yang, L. F., D. P. Xie, Z. B. Yuan, Z. J. Huang, H. B. Wu, J. L. Han, L. J. Liu, and W. C. Jia, 2021: Quantification of regional ozone pollution characteristics and its temporal evolution: Insights from identification of the impacts of meteorological conditions and emissions. *Atmosphere*, **12**, 279, https://doi.org/10.3390/atmos12020279.

Yang, Y., H. Liao, and J. Li, 2014: Impacts of the East Asian summer monsoon on interannual variations of summertime surface-layer ozone concentrations over China. *Atmospheric Chemistry and Physics*, **14**, 6867–6879, https://doi.org/10.5194/acp-14-6867-2014.

Yu, Y. J., Z. Wang, T. He, X. Y. Meng, S. Y. Xie, and H. X. Yu, 2019: Driving factors of the significant increase in surface ozone in the Yangtze River Delta, China, during 2013–2017. *Atmospheric Pollution Research*, **10**, 1357–1364, https://doi.org/10.1016/j.apr.2019.03.010.

Zhao, Y. B., K. Zhang, X. T. Xu, H. Z. Shen, X. Zhu, Y. X. Zhang, Y. T. Hu, and G. F. Shen, 2020: Substantial changes in nitrogen dioxide and ozone after excluding meteorological impacts during the COVID-19 outbreak in mainland China. *Environmental Science & Technology Letters*, **7**, 402–408, https://doi.org/10.1021/acs.estlett.0c00304.

Zhao, Z. J., and Y. X. Wang, 2017: Influence of the West Pacific subtropical high on surface ozone daily variability in summertime over eastern China. *Atmos. Environ.*, **170**, 197–204, https://doi.org/10.1016/j.atmosenv.2017.09.024.

Zhao, Z. Z., Z. M. Zhou, A. Russo, H. D. Du, J. Xiang, J. P. Zhang, and C. J. Zhou, 2021: Impact of meteorological conditions at multiple scales on ozone concentration in the Yangtze River Delta. *Environmental Science and Pollution Research*, **28**, 62 991–63 007, https://doi.org/10.1007/s11356-021-15160-2.

Zheng, B., and Coauthors, 2018: Trends in China's anthropogenic emissions since 2010 as the consequence of clean air actions. *Atmospheric Chemistry and Physics*, **18**, 14 095–14 111, https://doi.org/10.5194/acp-18-14095-2018.

Zhong, Q. R., and Coauthors, 2018: Distinguishing emission-associated ambient air $PM_{2.5}$ concentrations and meteorological factor-induced fluctuations. *Environ. Sci. Technol.*, **52**, 10 416–10 425, https://doi.org/10.1021/acs.est.8b02685.

Zhou, D. R., and Coauthors, 2013: Impacts of the East Asian monsoon on lower tropospheric ozone over coastal South China. *Environmental Research Letters*, **8**, 044011, https://doi.org/10.1088/1748-9326/8/4/044011.